Volume 1 | Number 1 | Jan 2013 | Pages 1–100

MedChemComm

www.rsc.org/medchemcomm

pDOS

ROYAL SOCIETY OF CHEMISTRY

www.rsc.org/medchemcomm

ARTICLE TYPE

Design, synthesis and evaluation of QD-DTC-BisBiotin Nanobioconjugate as a potential Optical-SPECT imaging agent

Narmada Bag [a, b], Rashi Mathur[a,]*, Sweta Singh[a], Firasat Hussain[b], Ram Prakash Chauhan[c], Krishna Chuttani[a], Anil Kumar Mishra[a,]*

5

The biomedical application of semiconductor quantum dots (QDs) are still limited due to the decrease in their photoluminescence (PL) after surface modification for target specificity and in vivo imaging. This is
10 being taken care of by choosing ligands which can enhance the tumour specificity without affecting the optical properties of the core QDs. In this study we have synthesized dithiocarbamate (DTC) derivatised BisBiotin ligand (DTC-BisBiotin) and then functionalized it covalently over CdSe/ZnS quantum dot surface to produce (QD-DTC-BisBiotin) nanobiocojugate. The influence of the size of QD nanobioconjugate (10-15 nm) and optical properties are evaluated by TEM, UV-VIS and fluorescence
15 spectroscopy and have been found to be favourable for diagnostic imaging studies. The synthesized nanobioconjugate was further studied for its in vivo biodistribution and pharmacokinetics through a pre-targeting approach. In vivo pharmacokinetics and biodistribution studies were performed by radiolabelling the QD nanobioconjugate with [99m] Technetium ([99mTc]QD-DTC-BisBiotin). [99mTc]QD-DTC-BisBiotin showed significantly higher tumour uptake (5% ID/gm) with better tumour retention, high
20 tumour/normal organ contrast and enhanced pharmacokinetics as compared to native DTC-BisBiotin ligand. This illustrates that although bivalent effect of BisBiotin ligand is responsible for the tumour uptake, the Enhanced Permeable and Retention (EPR) effect due to the size of the QD nanobioconjugate plays a major role in the enhanced pharmacokinetics and biodistribution. The efficient binding of [99m] Tc with the QD nanobioconjugate also highlights its use as "a SPECT-optical imaging agent".

25 ## Introduction

Quantum dots have been exhaustively studied for biomedical applications ranging from clinical diagnosis to biological labelling .[1-11] Typically in the colloidal CdSe/ZnS QDs, cadmium cores are coated with a shell of higher energy band gap material
30 i.e. ZnS to enhance the quantum yield (QY) and to protect the core from oxidation and leaching of toxic cadmium ion. However the bare QDs do not possess biocompatibility to interact with biological system and are highly toxic. As compared to the organic dyes one of the key features to the successful application
35 of QDs in biosystem is the ability to tailor their surface properties with suitable ligands to achieve hydrophilicity, aqueous stability, targeting to specific tissues and organelles.[12-16]

Numerous ligands and strategies have been developed in recent years for preparing the biocompatible QDs nanobioconjugates.
40 Despite the significant advances in the methods of preparation, the performance of the ligand that binds to the surface site is a major deciding factor for optical imaging. These ligands give stability to nanocrystal in aqueous solvent and provide efficient electronic passivation that in turn leads to an expected to high
45 luminescence quantum yield. Most widely used strategies for

preparing QD bioconjugates are based on the substitution of native hydrophobic ligand by thiol containing compounds, like dihydrolipoic acid (DHLA), mercaptopropionic acid (MPA), mercapto acetic acid (MAA), cysteine, cysteamine, penicillamine,
50 etc. which can interact strongly with quantum dot surface due to dynamic SH-ZnS interactions.[16-24] However thiol conjugated quantum dots are photochemically unstable due to photocatalytic oxidation, photoxidation and precipitation of the nanocrystal of ligands.[25] Some histidine expressing proteins and peptides have
55 also been used as ligands which use metal affinity coordination for binding with the QD surface.[26-28] Other ligands such as cationic multivalent polyamines use ion exchange method for capping the QD surface.[29]However all these approaches require either multistep synthetic procedures or oxygen-sensitive
60 chemical to obtain the final QD conjugates resulting in loss of quantum yield. Earlier researches have shown strong indications of dithiocarbamate (DTC) a bidentate chelating molecule, as a potential ligand for the development of water soluble colloidal core shell quantum dots as it can preserve the desirable optical
65 properties due to the higher binding energy and affinity for the metal atoms.[30-33] Although it is obvious that there will be reduction in quantum yield of hydrophobic QDs as they undergo

phase transfer i.e. organic to aqueous environment but DTC stabilized CdSe/ZnS QDs show a higher quantum yield as compared to the other ligands. For specific targeting we need to attach these novel DTC ligand with biomolecule to make
5 inorganic semiconducting QDs biocompatible and target specific.

There are various approaches that have been reported earlier for targeted tumour imaging, among which Biotin-Avidin system has been very useful , this is because avidin can bind very
10 efficiently to the tumour sites because of its good degree of glycosylation and high isoelectric point of about 10.5.[34-35] Secondly the interaction of avidin with biotin and biotinylated agents is known to be the strongest non covalent interaction which not only involves very rapid bond formation but also once
15 formed are very stable over wide range of temperature (up to 120^0C), pH (2-13), organic solvents and denaturing agents. Additionally, the high affinity of avidin for biotin with a dissociation constant of the order of 10^{-15} M, which is about one million times greater than most antigen antibody interaction and
20 the ability of one avidin molecule to bind with four biotin units helps to increase the accumulation of biotinylated nanoparticles to the tumour site. The use of pre-targeting approach which involves the intravenous introduction of avidin before injecting the biotinylated compound in the body results in the improved
25 target-to-nontarget ratio.[36-38] In the present work we have used DTC-BisBiotin ligand to generate specificity on the QDs using the pre-targeting approach however, our main objective is to evaluate the effect of QDs on the pharmacokinetics and biodistribution pattern of the QD nanobioconjugate as compared
30 to the native DTC-BisBiotin ligand.

Herein, we have designed and synthesized new stable colloidal biotinylated CdSe/ZnS QDs utilizing the DTC-bis (3-propylamine) ligand appended with two molecules of biotin. In an attempt to synthesize biotin functionalized QDs, novel Bis-
35 Biotin analogue was synthesized by reacting Biotin-NHS-ester with Bis(3-aminopropylamine), then its DTC analogue was grafted on the synthesized CdSe/ZnS QDs. The most important aspect in synthesizing the Bis-Biotin molecule is to maintain the optimum amount of ligand density. It means with the small
40 number of ligands grafted to the quantum dot surface the biomolecule loaded would be double, which would result in an increase in the uptake at tumour site. However as the steric ligand packing density can be minimized so the quantum yield is not much affected. The surface coordination of the above mentioned
45 ligand preserves the required luminescence of the nanocrystal and aqueous stability in addition to being stable for weeks without any precipitation. The synthesis of the ligand and its conjugation to the quantum dot surface has been characterized by mass spectrometry, NMR spectroscopy, UV-Vis spectroscopy,
50 transmission electron microscopy (TEM) and live cell fluorescence imaging. The fluorescence studies show that QD-DTC-BisBiotin can be used as a potential optical imaging agent. The designed nanobioconjugate can be used as a SPECT imaging agent as it can be radiolabeled with technetium (^{99m}Tc). This
55 technique is very helpful in evaluating the biodistribution and pharmacokinetics of these nanocrystals which would otherwise be difficult with fluorescence imaging.

RESULT AND DISCUSSION

Synthesis of ligand

60 The chemical structure and synthetic procedure for the synthesis of the bifunctional DTC-BisBiotin ligand is illustrated in (scheme-1). The BisBiotin ligand was synthesized in 3 steps. In the first step biotin was converted to biotin-NHS-ester (1) using N-hydroxysuccinimide in the presence of
65 dicyclohexyledicarbodimide (DCC). Further Biotin-NHS was reacted with Bispropylamine to form 5-(2-Oxo-hexahydro-thieno [3, 4-d] imidazol-6-yl)-pentanoic acid (3-{3-[5-(2-oxo-hexahydro-thieno [3, 4-d] imidazol-6-yl)-pentanoylamino}-propyl)-amide (BisBiotin) (2). The desired bifunctional DTC-Bis-
70 biotin (3) was finally obtained by mixing CS_2 and Bis-biotin in the presence of KOH in DMF. The synthesized ligand was characterized by ^{1}H NMR, ^{13}C NMR, ESI-MS and UV-Vis spectroscopy. ^{1}H NMR shows the characteristic peaks of biotin and the characteristic three multipletes of bispropylamine residue
75 i.e. at 1.8, 3.1 and 4.0 ppm. In ^{13}C NMR spectrum peak at 176 ppm confirms the amide bond formation while the peak at 179 indicates the quaternary dithiocarbamate carbon (Fig. 2). Synthesis of DTC-BisBiotin was further confirmed by mass spectrometry with peak at 659.2 corresponds to (M+H$^+$) and
80 elemental analysis. The formation of dithiocarbamate derivatised BisBiotin was also verified by UV-Vis spectroscopic studies. The characteristic absorption peak of CS_2 (310 nm) disappeared completely from DTC-BisBiotin and concomitant appearance of two new absorption peaks at 260 and 290 nm characteristic of
85 dithiocarbamate due to π-π* transition and n-π* transition respectively (Fig. 3). Here we have tried to synthesize a bis biomolecule conjugated ligand, so that we are able to conjugate large number of biomolecules with a small number of ligand grafted on the quantum dot surface. This would lead to minimize
90 the steric ligand packing density over the nanocrystals surface and to preserve the luminescence. Once the ligand was successfully synthesized its conjugation with the QDs is important.

Surface functionalisation of quantum dots with ligand

95 Organic phase synthesis of quantum dots produces high quality hydrophobic QDs which are soluble in non-polar organic solvents like chloroform, toluene and hexane. However, for biological system QDs must be made water soluble. Generally solubility in water should yield nanocrystals which are soluble and stable in
100 biological buffer with preserved photophysical properties and relatively small particle size. There are mainly two extra processing steps reported to produce water soluble QDs which satisfy these criteria. One approach is indirect surface encapsulation which involves a hydrophobic-hydrophobic
105 interaction between the hydrophobic section of polymers and stabilizing agents present on the surface of QDs. This method produces extremely water soluble QDs with preserved optical properties because coating does not directly interact with QDs surface and does not disturbs passivation layer. However this
110 method results in dramatic increase of the nanocrystal hydrodynamic size which is unfavourable for biological imaging and also reduces the intracellular penetration of QDs. The other approach is that of ligand exchange which involves replacing the hydrophobic surface ligand with a hydrophilic one. This process

is ideal for the synthesis of water stabilized QDs by using small molecular weight molecule which suppress the non-radiative decay of the excitons providing stability and biocompatibility.
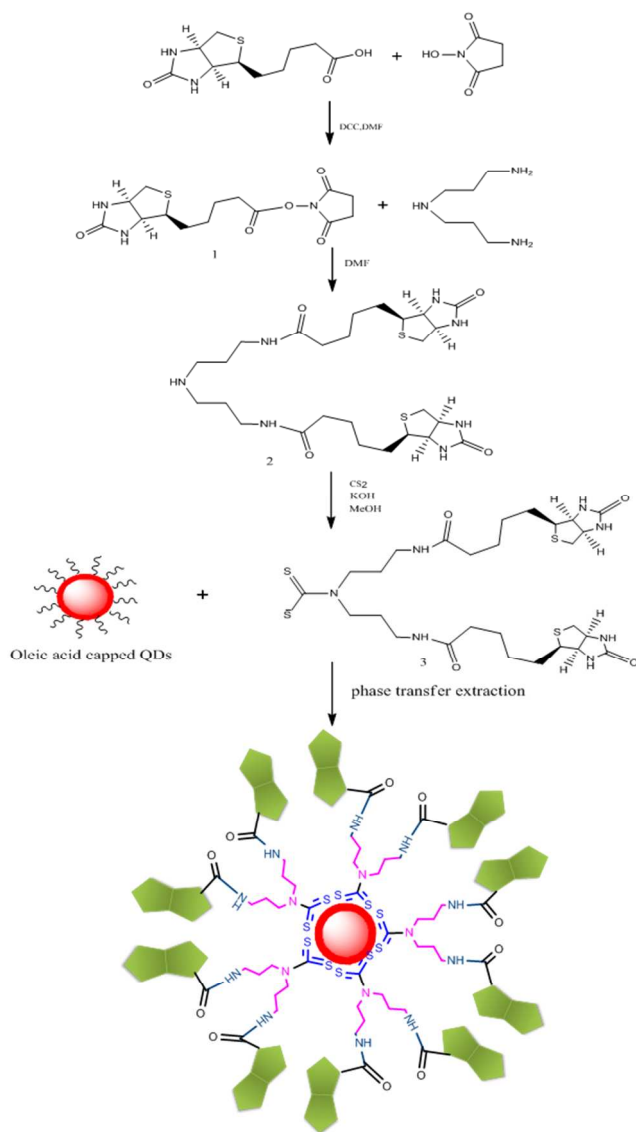
Scheme. 1 Synthetic scheme of QD-DTC-BisBiotin

In the present work we have used the ligand exchange method for solubilisation of red light emitting quantum dot having a characteristic absorbance at 590nm. The successful ligand exchange process was carried out by a biphasic reaction where the QDs were soluble in chloroform and the ligand was soluble in water. We found that the biphasic exchange was much more efficient using chloroform as the organic phase solvent rather than toluene and hexane. Biphasic ligand exchange was facilitated by vigorous stirring and sonication which may be responsible for enhanced contact between two immiscible solvent. DTC derivatised ligand was able to displace the native hydrophobic group (oleic acid).The obtained DTC-BisBiotin ligand shows good results for the phase transfer of hydrophobic

QDs to the aqueous phase. In the above described procedure the exchange was completed in almost 6-8 hrs.
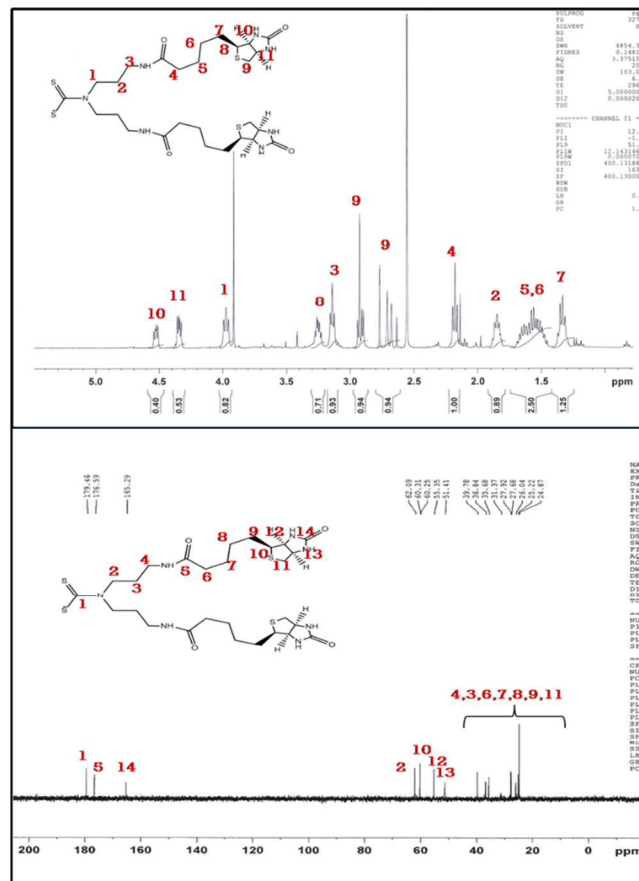

Fig. 2 (1) ^{1}H NMR spectra of Bis– (3-(5-(2-oxo-hexahydro-thieno (3, 4-d) imidazole6-yl)-pentanoyleamino)-propyl) - dithiocarbamicacid, (2)^{13}CNMR spectra
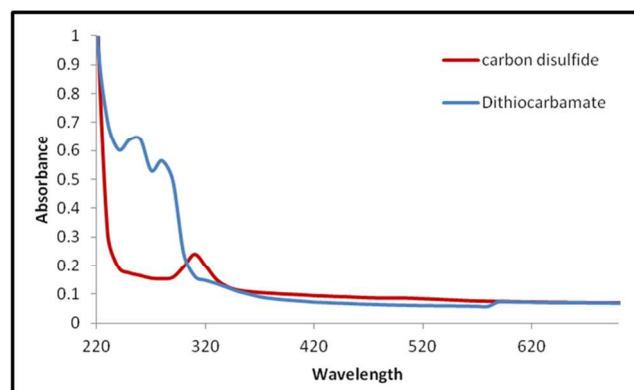

Fig. 3. UV-VIS absorbance spectrum of DTC-Bisbiotin and carbon disulphide

The exchange reaction was monitored throughout the process spectroscopically. Initially we get three peaks at 260 nm, 290 nm and 590 nm. The completion of the reaction is indicated by the presence of two peaks at 290 and 590nm instead of three i.e. peak at 260 nm disappears which is a strong evidence of conjugation of DTC ligand to the QDs surface (Fig. 4). The peak at 260nm is attributed to π-π* transition of DTC ligand which disappears after conjugation with QDs. The UV-Vis absorption spectra of QDs in

QD-DTC-Bisbiotin (in water) remain unchanged in comparison with the original hydrophobic QDs (in chloroform) on phase transfer. Interestingly the size of the nanocrystals (10-15 nm) is also not affected much by the surface modification as shown by the TEM (Fig.5). There is no change in the position of the fluorescence peak of QD-DTC-Biotin compared to the as synthesized hydrophobic QDs in chloroform. This clearly indicates that the ligand exchange process used for synthesizing the biocompatible QD-DTC-BisBiotin does not influence the basic optical properties of the core shell CdSe-ZnS QDs (Fig.6). Interestingly, water soluble QD-DTC-BisBiotin maintained the high fluorescence quantum yield of the original hydrophobic QDs dispersed in organic medium while in previous report, loss of fluorescence brightness of QD undergoing phase transfer into aqueous medium was reported.[25] In case of thiol ligands, both electron-hole recombination process and disulphide bond formation are responsible factors for the low quantum yield after phase transfer. Thiols generally generates thiolate ions in aqueous solution which may introduce new hole trap states at high concentrations that lead to dramatic decrease in the fluorescence intensity. In the present work dithiocarbamate which is the anchoring group on the QDs surface neither forms the disulphide bond nor the thiolate ion.[33] This may be the partial explanation why the quantum yield of these QDs remains constant before and after phase transfer.
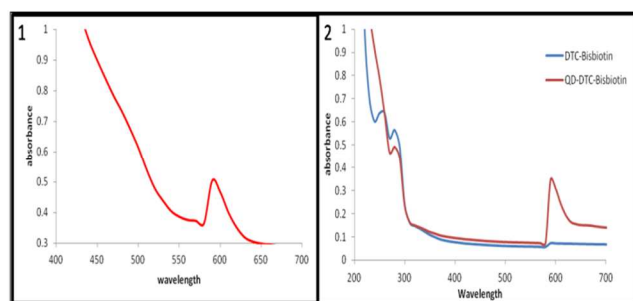

Fig. 4 (1) UV-VIS absorbance spectrum of (1) red light emitting QDs (2) DTC-Bisbiotin and QD-DTC-Bisbiotin
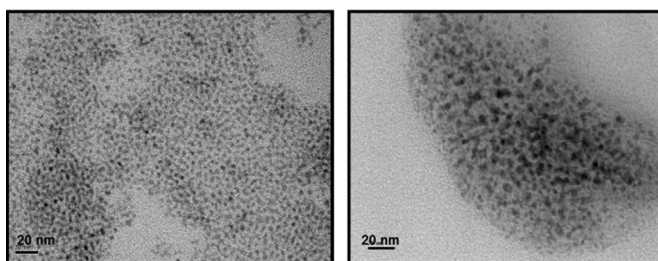

Fig.5 TEM images of CdSe/ZnS quantum dots before and after surface modification. (1) CdSe/ZnS QDs in chloroform, (2) QD-DTC-Bisbiotin in water

Fluorescence studies

The fluorescence studies of these quantum dot bioconjugates in Chinese hamster ovarian cell line showed no uptake of the QDs within a couple of hours of incubation. However after 16 hrs of incubation small amount of QDs were found to be present in the internal periphery of the cells (Fig.7). As we have taken the noncancerous cell line the uptake is very slow and the QDs which do internalize are due to the size and charge dependent endocytosis. The leaky vasculature of the tumour cells would enhance this uptake as is evident from the biodistribution studies.
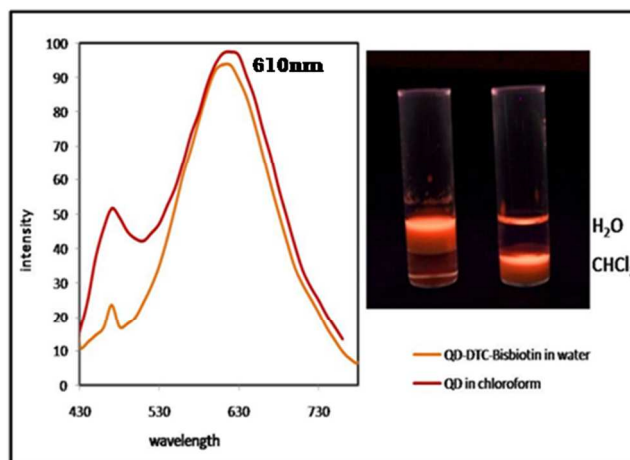

Fig. 6 (1) Fluorescence spectra of QD and QD-DTC Bisbiotin (2) Biphasic extraction of QDs from chloroform to water
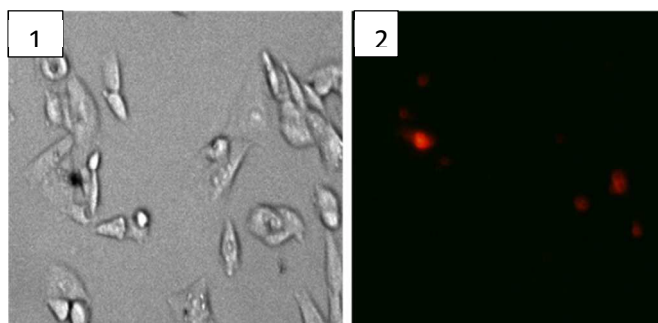

Fig. 7 Fluorescence image of QD-DTC-BisBiotin in AA8 chinese hamster ovarian cell line (CHO) after 16 hrs. of incubation (1) Bright field (2) Fluorescence.

In vitro Stability

DTC-Bisbiotin and QD-DTC-Bisbiotin were labelled with 99mTc. All the labelling parameters such as pH, concentration of reducing agents (SnCl2), temperature, etc. were standardized to achieve the maximum labelling efficiency. The proteolytic degradation of the radiolabeled nanobioconjugate was determined in human serum in vitro. ITLC analysis of the human serum revealed that the 99mTc-DTC-Bisbiotin and 99mTc QD DTC-Bisbiotin remained sufficiently stable during incubation at 37°C with human serum. A maximum of 5-6% of radioactivity degraded after 24 hrs of incubation advocating a high in vitro stability of almost 94-95% of the QD-DTC-Bisbiotin for up to 24 hrs (Fig.8).
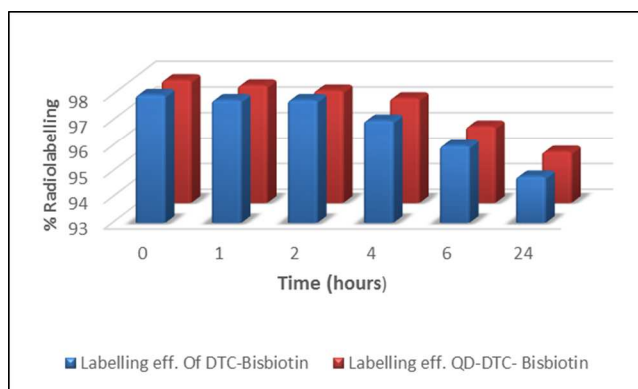
Fig.8 In vitro serum stability study of DTC-Bisbiotin and QD-DTC Bisbiotin

Blood kinetics

The in vivo blood clearance kinetics was performed in rabbits and results showed that radiolabeled nanoconjugate shows a biphasic clearance (Fig. 9).The calculated value for $t_{1/2(fast)}$ indicate that the clearance of QD nanobioconjugate from the blood and distribution to the various organs is 90 mins. With passage of time its clearance rate became slow and the $t_{1/2\ (slow)}$ is 355 minutes. This indicates the internalisation of the QD nanobioconjugate in the various organ. It is evident from the blood kinetics that even after 24 hrs (2%) activity remains in the blood circulation.
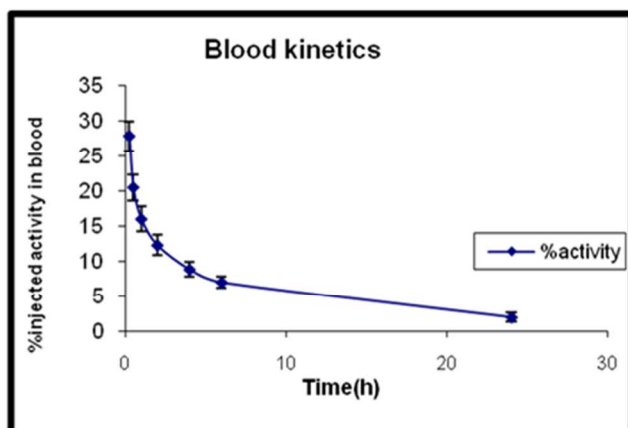

Fig.9 Blood clearance profile of ^{99m}Tc labelled QD-DTC-BisBiotin

Biodistribution and scintigraphy studies

According to previous reports quantification and tracking of QDs in vivo is limited with fluorescence imaging because visualization of fluorescent QDs from deeper tissue is difficult. To address this issue research has been carried out by conjugating DOTA-^{64}Cu with QDs surface and their biodistribution in vivo has been studied by micro PET based imaging.[41-42]For accurate quantification of tumour targeting efficiency dual modality probe for both fluorescence and magnetic resonance imaging (MRI) have been developed recently.[43-45]Here we have evaluated the pharmacokinetics of the QD nanobioconjugate and the synthesized native DTC-BisBiotin ligand by SPECT imaging technique. As the DTC-BisBiotin has many sites available for binding ^{99m}Tc, the percentage radiolabeling of the nanobioconjugate was found to be more than 98%. The biodistribution and pharmacokinetic studies of DTC-BisBiotin ligand and QD-DTC-BisBiotin were done after radiolabelling with ^{99m}Tc and pre-targeting with avidin.

It has been reported earlier that high accumulation of biotinylated nanoparticle is found in liver, kidney and spleen due to large number of macrophages present in MPS system, negative charge present on the biotinylated nanoparticle at physiological pH and rapid clearance of the avidin from blood circulation.[46-48] QDs predominantly accumulate in liver and spleen by reticuloendothelial system (RES). However when modified with PEG and antibody, QDs are taken up by tumour site due to EPR effect and antibody-antigen active targeting with reduced non-specific accumulation in RES system.[49]The present study demonstrates that the DTC-BisBiotin ligand shows a significant tumour uptake (5%ID/gm) due to the bivalent effect of biotin which is expected. The uptake in the liver (17% ID/gm), spleen (5%ID/gm), and kidney (10% ID/gm) is also quite high and the amount in blood is (2%ID/gm). However as soon as the QD is attached to the ligand interesting changes are observed in the biodistribution pattern. The uptake in the liver (5%ID/gm), spleen (2.5%ID/gm) and kidney (5%ID/gm) shows a dramatic decrease while the uptake in the lungs (4.5%ID/gm) and blood (5%ID/gm) increases (Fig.10). Although in this system we have not used any PEG or antibody, still there is a dramatic decrease in the non-specific uptake of QD-DTC-BisBiotin in RES system. This change in pharmacokinetics may be due to the size effect of QDs and the surface modifications made there on. However when we compared the tumour uptake in both the cases we found that tumour uptake in case of QD-DTC-BisBiotin is marginally high than the native ligand. This indicate that the specific targeting is achieved due to the bivalent effect of BisBiotin ligand however the conjugation of QDs modifies the pharmacokinetics resulting in faster wash out of QDs from the other organs. This results in an enhanced target to non-target ratio improving the contrast as evidenced from the scintigraphy images (Fig. 11).We see the tumour to muscle ratio remains the same in both the cases while the tumour to liver ratio changes dramatically. This is also evident from the scintigraphic images in which the activity retained at tumour site in QD-DTC-BisBiotin is higher than DTC-BisBiotin alone.
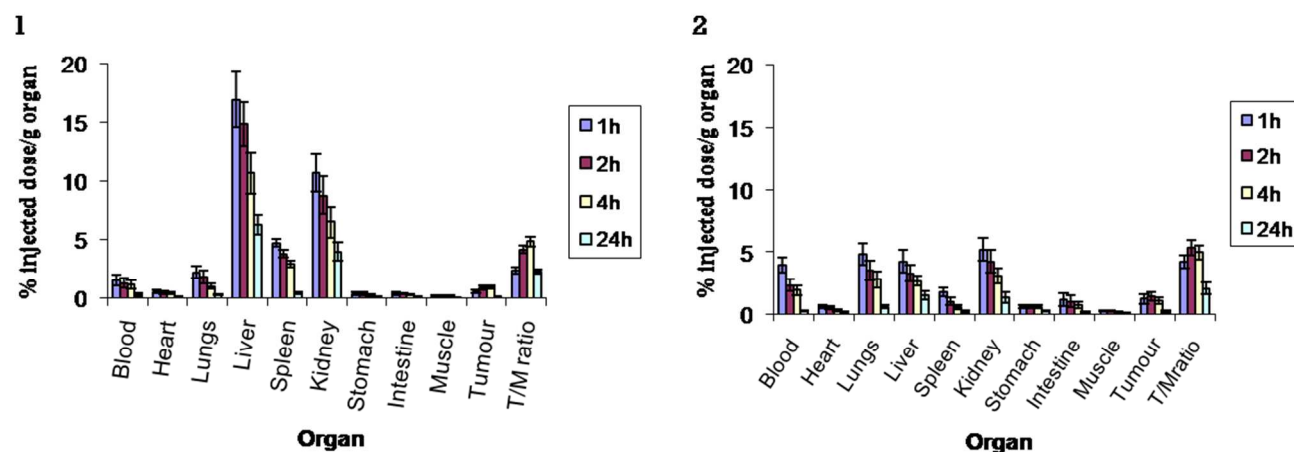
ARTICLE TYPE

Fig.10 Biodistribution pattern of ^{99m}Tc labelled (1) native DTC-BisBiotin, (2) QD-DTC-BisBiotin

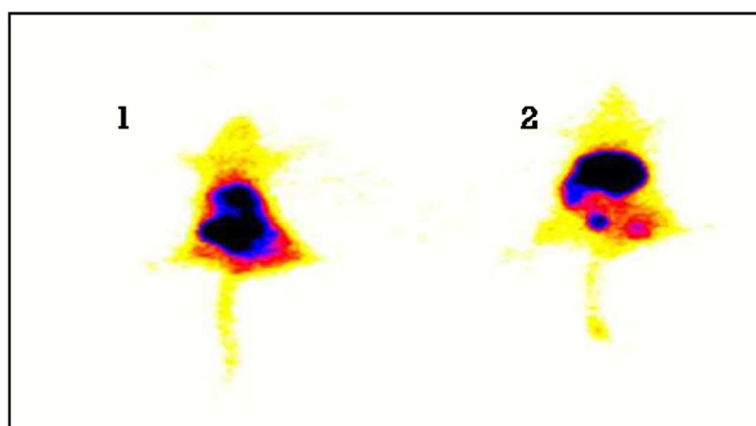**Fig.11 S**cintigraphy image of mice showing uptake of ^{99m}Tc labelled (1) DTC-BisBiotin (2) QD-DTC-BisBiotin

CONCLUSION

We have successfully designed and synthesized a new dithiocarbamate Bis-Biotin derivative and appended on the surface of quantum dots. The synthesis technique is very facile and gives water soluble, target specific and biocompatible QDs in good yield for tumour imaging.   The synthesis procedure also helps us in optimizing the ligand density on the quantum dot surface so that the fluorescence properties of the quantum dots are retained even after phase extraction of the corresponding oleic acid capped quantum dots. The dithiocarbamate ligand is not only responsible for the stability of these quantum dot based nanobioconjugates in aqueous solution but also helps in doubling the amount of biomolecule on each ligand molecule and hence the specificity. The surface groups on nanobioconjugate form a stable complex with ^{99m}Tc which helps in studying the pharmacokinetics and also show the ability of this nanobioconjugate to act as an efficient SPECT imaging agent.

The major role played by the QDs in modifying the in vivo distribution and kinetics, contributes significantly in improving the target to non-target ratio and hence enhancing the contrast. This nanobioconjugate therefore can be of clinical relevance as it has the ability to combine the goodness of optical imaging i.e. high spatial and temporal resolution and SPECT imaging i.e. sensitivity in depth.

Experimental details

Synthesis of Biotin-NHS-ester-(1)

NHS-ester of Biotin was synthesized according to earlier reported method.[39] Briefly, Biotin (4.09 mmol) was dissolved in dry DMF (25 ml) under inert atmosphere at 40^0 C. After stirring the solution for 10 mins, dicyclohexylcarbodimide (4.09 mmol) was added followed by N-Hydoxysuccinimide (5.0 mmol). The reaction was left overnight for stirring and the completion of the reaction was checked by TLC (9:1 dichloromethane: methanol). Then the reaction mixture was filtered to remove the dicyclohexylurea and evaporated to dryness. The crude compound was precipitated with diethyl ether to give 1 (Biotin-NHS- ester) the required product as white powder in good yield (90%). ^{1}H NMR (DMSO-d_6, 400 MHz) : δ (ppm), 1.52-1.60 (m,2H), 1.62-1.93(m,4H), 2.58-2.70 (m,2H), 3.03-3.15 (m, 2H), 3.37 (s,4H), 3.40-3.51(m, 2H), 4.01-1.19 (m,1H), 4.21-4.32(m, 2H), 6.40-6.70 (m, 2H, -NH); ^{13}C NMR (DMSO-d_6, 100 MHz), : δ (ppm) 24.76, 25.89, 28.29, 30.46, 32.23, 36.25, 55.70, 59.66, 61.48, 163.20, 169.40, 170.75.   Mass m/z (ESI) calculated for $C_{14}H_{19}N_3O_5S$, 341found 342.2 (M +H^{+}).

Synthesis of Bisbiotin-2

Biotin-NHS-ester, 1 (2.93 mmol) was added to 30 ml of dry dimethyl formamide along with N^1 – (3-Amino-propyl)-propane - 1, 3-diamine (1.40mmol) under inert atmosphere. The resulting solution was left for stirring at room temperature for 24 hrs. After stirring the solution was filtered and evaporated to dryness. The appearance of the resulting compound 2 was colourless and sticky (900mg). ^{1}H NMR (D_2O, 400MHz) : δ (ppm), 1.29 (m, 4H ,CH_2), 1.57 (m, 4H), 1.62-1.67 (m, 8H ,-CH_2), 2.18 (t, 4H,-CH_2), 2.55 (t, 4H, -CH_2), 2.97 (t, 4H , -CH_2), 3.20 (t, 4H , CH2), 3. 36 (m, 2H , -CH), 4.59 (t, 2H, -CH-NH), 4.60 (t, 2H , -CH-NH) , 6.5 (s, 4H , NH) ; [13] CNMR (D_2O , 100 MHz) ; δ (ppm), 25.6, 26.0, 30.2, 34.3, 33.6, 36.4, 40.5, 46.6 (-CH2), 48.4, 48.9 (-CH), 163.2, 174.7 (-CO);   m/z (ESI) calculated for $C_{26}H_{45}N_7O_4S_2$ 583.2., found 585.3 (M +2H[+]).

Synthesis of DTC-Bisbiotin-3

The compound 2 (1.20 mmol) was dissolved in 20 ml dry methanol along with potassium hydroxide (4.81 mmol) at -10^0 C. After stirring for 10 min carbon disulphide (4.819 mmol) in methanol was added drop wise and the resulting solution was left for stirring at room temperature overnight. The resulting solution was filtered and evaporated to dryness and then recrystallised with diethyl ether. The appearance of the compound 3 was yellow solid (545.0 mg). ^{1}H NMR (D_2O,400MHz) : δ (ppm) , 1.33-1.38 (m, 4H ,CH_2), 1.50-1.67 (m, 8H,-CH_2), 1.86 -1.87 (m, 4H, -CH_2), 2.18 (t, 4H, -CH_2), 2.68-2.95 (dd, 2H , -CH_2), 3.13 -3.16 (t ,4H ,-CH_2), 3.24-3.27 (m , 2H , -CH_2), 3. 96-4.00 (t , 4H ,-CH_2), 4.33-4.36 (m, 2H, -CH-NH) , 4.51-4.53 (m , 2H , -CH-NH

) ;   [13] C NMR (D2O, 100 MHz) ; δ (ppm), 25.6, 26.0 , 30.2 ,34.3 ,33.6 ,36.4 , 40.5,   46.6 (-CH2) ,48.4 ,48.9 (-CH) ,163.2,174.7 (-CO),209.3 (-CS) ;   m/z (ESI) calculated for $C_{27}H_{44}N_7O_4S4$ 658, found 659.2 (M + H^{+}). The calculated value for elemental analysis was C = 49.2%, H = 6.73%, N = 14.88%, O = 9.71%, S = 19.46% and the observed values are C = 49.62%, H = 7.13%, N = 14.20%, O = 9.29%, S= 20.06%.

Synthesis of CdSe/ZnS quantum dots

Here we have used red light emitting quantum dots which were synthesized by the protocol reported earlier with some modification.[40] Briefly CdSe core quantum dots were synthesized by using oleic acid both as solvent and capping agent. In a three neck round bottom flask containing cadmium acetate (1M) and oleic acid purged with dry nitrogen gas was heated up to 190^0C. Selenium powder was mixed with TOP and sonicated for approximately 10 mins. This was rapidly injected into the reaction chamber with syringe and stirred vigorously. After getting the core quantum dot of desired size indicated by the colour change the temperature was suddenly lowered to less than 100^0C to introduce a ZnS shell over the core surface. Then the Zn and S precursor (zinc acetate and hexadimethylesilathiane) were added in the reaction mixture simultaneously under stirring. The resulting oleic acid capped CdSe/ZnS core shell QDs were precipitated and re-dispersed in chloroform to remove uncapped ligands. Further the QDs of desired size and colour were purified by size selective precipitation method. The synthesized nanocrystals were characterized by UV and TEM (Fig. 4).

Biphasic ligand exchange procedure

The synthesized oleic acid capped red CdSe/ZnS quantum dots, size ~ 5-6nm, excitation maxima at 590nm and emission maxima at 610 nm are stable and soluble in chloroform. 5ml of (0.7 μM) solution of quantum dots was prepared in chloroform. DTC-BisBiotin ligand ($9.8x10^{-2}$ M) was prepared in 5 ml of PBS buffer with a pH 7.4. Both the solution are mixed in a round bottom flask and kept for vigorous stirring over a magnetic stirrer. After 24 hrs all the hydrophobic QDs were found in water layer which is a strong indication for the successful phase transfer ligand exchange reaction. The reaction was also confirmed from the UV-Vis studies. The aqueous layer was then separated from the organic layer by centrifugation. The supernatant containing excess of free ligands was removed and the QD-DTC-BisBiotin abstracted as pellet was dissolved in PBS buffer. The nanocrystals are stable in aqueous media over several weeks at 4^0 C without formation of precipitates.

Cell culture and fluorescence microscopy

AA8 Chinese hamster ovarian cell line (CHO) were grown and maintained in minimum essential medium (low glucose DMEM), with 10% fetal bovine serum (FBS). Then the cell were trypsinized with 0.05% trypsin in a 60-mm culture plate and incubated for 2 min. After incubation the trypsin was decanted and kept at 37 ^{0}Cfor 30 sec to 1 min. As soon as cell gets detached from the culture plate, DMEM media was added and a homogeneous suspension was made. Then the suspension was divided and transferred to a 35-mm culture plate which contains approximately $1x 10^6$ cells /ml. These plates were then kept in an

incubator at 37 ^{0}C with 5% CO_2. After 36 hrs of incubation finally 100 µl of QD biotin conjugates was added and mixed properly. The plates were returned to the incubator, taken out after each specific time interval and imaged under live cell imaging microscope.

In vitro serum Stability

The metabolic stability of the DTC-Bisbiotin and QD-DTC-Bisbiotin was ascertained in vitro in freshly collected human serum from healthy volunteers (prior informed and consent taken). Human serum was prepared by allowing blood collected from healthy human volunteers to clot for 1hr at 37°C in a humidified incubator maintained at 5% carbon dioxide, 95% air. The samples were then centrifuged at 400 g and the serum was filtered through a 0.22 µm filter into sterile plastic culture tubes. 100 µL of 99mTc labelled formulations were incubated respectively in 900 µL of this serum (in duplicate) at 37°C and analysed to check for any dissociation of the complex by ITLC using silica gel strips and 0.9% NaCl aqueous solution (saline) as developing solvent. The change in labelling efficiency was monitored over a period of 24 hr.

Radiolabeling

An aqueous solution of QD-DTC-BisBiotin (9.78 nmol) was taken in a shielded vial and stannous chloride was added. The pH of the resulting solution was adjusted to 6.5-7.0 with 0.5 M $NaHCO_3$. Then the mixture was passed through a 0.22 µm Millipore filters into a sterile vial. Freshly eluted $^{99m}TcO_4^-$ (93.7MBq) was added and the complex was incubated for 30 min at room temperature for optimum labelling yield. The labelling efficiency was estimated chromatographically using ITLC-SG as the stationary phase and 100% acetone as mobile phase. The paper chromatography demonstrated absence of unbound $Na^{99m}TcO_4$.

Blood kinetics and Biodistribution

All animal experiments and study protocols were approved by the Committee for the Purpose of Control and Supervision of Experiments on Animals (CPCSEA), Government of India, New Delhi. Animal handling and experimentation was carried out as per the guidelines of the Institutional Animal Ethics Committee.
Blood clearance of 99mTc-labeled nanobioconjugates was studied in healthy New Zealand Albino rabbits weighing 2.5-3.5 kg (n = 3). 600µCi of the radiolabelled complex in saline was administered intravenously through the dorsal ear vein which were preinjected with avidin. Blood samples were withdrawn from the other ear vein at different time intervals ranging from 5 mins-24 h. Persistence of activity in the circulation was calculated as percentage injected dose per whole blood, assuming total blood volume as 7% of the body weight. The radioactivity of the precipitate and supernatant was measured in a well-type gamma spectrometer.
Tumour bearing BALB/c mice with EAT grafted tumour in right thigh were used. The mice were administered 100 µCi of 99mTc labelled nanobioconjugate, respectively, through the tail vein (i.v.). At 1, 2, 4 and 24 h post injection, the animals (n = 3) were euthanized and blood was collected by cardiac puncture into preweighed tubes. The mice were then dissected and different organs (heart, lungs, liver, spleen, kidneys, stomach, intestine,

muscle (normal and tumour) and brain) were removed, weighed and their radioactive counts taken with the help of a gamma counter. Uptake of the radiolabeled compound into each organ was measured per gram of the tissue/organ and expressed as percentage injected dose per gram organ weight. The radioactivity remaining in the tail (point of injection) was also measured and taken into account while calculating the radioactivity.

Scintigraphy

Scintigraphic studies were performed on a gamma camera. 100 µL of the radiolabeled DTC-BisBiotin and QD-DTC-BisBiotin conjugates was injected through tail vein of BALB/c mice. The tumour was inoculated in the right thigh of the mice using the EAT cell line.

Acknowledgements

Notes and references

^{a} *Department of Cyclotron and Radiopharmaceutical Sciences, Institute of Nuclear Medicine and Allied Sciences, Defence Research and Development Organization, Brig. S.K. Mazumdar Marg, New Delhi-110054, India*
^{b}*Department of Chemistry, Delhi University, New Delhi-110054, India*
^{c}*Department of Chemistry, SVGC Ghumarwin, Bilaspur, Himachal Pradesh-174021, India*
Corresponding authors:
E-mail address:*mrrp303@gmail.com (Rashi Mathur and Anil Kumar Mishra)*

1. I.L. Medintz, H.T. Uyeda, E.R. Goldman, H. Mattoussi, *Nat. Mater.*, 2005,**4**, 435-446.
2. Salmanogli,. *Cancer Nanotechnology,* 2011,**2**, 1-19 .
3. R.E. Bailey, A. M. Smith, S. Nie, *Physica. E.*, 2004, **25**, 1-12.
4. M. Smith, X. Gao, S. Nie, *Photochem. Photobiol.*,2004,**80**, 377 -385.
5. M. Bruchez, M. Moronne, P. Weiss, A. P. Alivisatos, *Science*, 1998, **28** , 2013 -2016.
6. W.C.W. Chan, S.M. Nie,. *Science*, 1998, **281**, 2016-2018.
7. P. Suriamoorthy, X. Zhang, G. Hao, A.G. Joly, S. Singh, M. Hossu, X. Sun, W. Chen, *Cancer Nano.*, 2010, **1**, 19-28.
8. H. Tada, H. Higuchi, T. M. Wanatabe, N. Ohuchi, *cancer research,* ,2007,**67**,1138-44.
9. R. L. Ornddorff, S. J. Rosenthal, *Nano. Lett.*,2009,**9(7),**2589-2599.
10. H. Chen, B.Li, M. Zhang, K. Sun, Y. Wang, K. Peng, M. Ao, Y. Guo, Y. Gu, *Nanoscale*, 2014,**6**,12580-12590.
11. K. Joo, Y. Fang, Y. Liu, L. Xiao, Z. Gu, A. Tai, C.L. Lee, Y. Tang, P. Wang, ACS Nano, 5(5),3523-3535.
12. P. Zrazhevskiy, M. Sena, X. Gao,. *Chem. Soc. Rev.*, 2010,**39**, 4326-4354.
13. U. R. Genger, M. Grabolle, S.C. Jaricot, R. Nitschke, T. Nann, *Nature Methods*, 2008,5,763-775.
14. Z. Yu,R. M. Schmaltz, T.C.Bozeman,R. Paul, M. J. Rishel,K. S. Tsosie,S. M. Hecht, *J. Am. Chem. Soc.*,2013,**135 (8)**,2883-2886.
15. C. Bhattacharya, Z. Yu, M.J. Rishel, S. M. Hecht, *Biochemistry*, 2014,**53(20)**,3264-3266.
16. J. A. Lines, Z. Yu, L.M. Dedkova, S. Chen, *Biochem Biophys Res Commun.*, 2014,**443(1),** 308-312.

17. H. Mattoussi, J.M. Mauro, E.R. Goldman, G.P. Anderson, V.C. Sundar, F.V. Mikulec, M.G. Bawendi,*J.Am. Chem. Soc.*, 2000, **122**, 12142-12150.
18. K. Susumu, H. T. Uyeda, I.L. Medintz, T. Pons, J. B. Delehanty, H. Mattoussi, *J.Am. Chem. Soc.*,2007, **129**, 13987-13996.
19. P. Kumar, D. Kukkar, A. Deep, S.C. Sharma, L. M. Bharadwaj,*Adv. Mat. Lett.*, 2012, **3**(6), 471-475.
20. Y. Zhang, A. Clapp,. *Sensors.*, 2011, 11, 11036-11055.
21. M. Koneswaran, R. Narayanaswami, *Microchim. Acta*. **178**, 171-178.
22. W. Liu, H. S. Choi, J. P. Zimmer, E. Tanaka, J. V. Frangioni, M. Bawendi, *j. Am. Chem. Soc.*, 2007, **129**, 14530-14531.
23. R. Kuang, X. Kuang, S. Pan, X. Zheng, J. Duan, Y. Duan, *Michrochim. Acta.*, 2010, **169**, 109-115.
24. G. J. Stasiuk, S. Tamang, D. Imbert, C. Poillot, M. Giardiello, C. Tisseyre, E. L. Barbier, P. H. Fries, M. D. Waard, P. Reiss, M. Mazzanti, *ACS Nano*. , 2011, **5**, 8193-8201.
25. J. Aldana, Y.A. Wang, X. Peng, *J.Am.Chem.Soc.,* 2001, **12**, 8844-8850.
26. E. R. Goldman, I. L. Medintz, A. Hayhurst, G. P. Anderson, J. M. Mauro, B. L. Iverson, G. Gergious, H. Mattoussi H.. *Analytical Chimica Acta.*, 2005,**534**, 63-67.
27. L. Medintz, A. R. Clapp, F. M. Brunel, T. Tietenbrunn, H. T. Uyeda, E. L. Chang,J. R. Deschamps, P. E. Dawson, H. Mattoussi, *Nat. Mater.*, 2006, **5**, 581-589.
28. J. B. Delehanty, I. L. Medintz, T. Pons, F. M. Brunel, P. E. Dawson, H. Mattoussi, *Bioconjugate Chem.*, 2006, **17**, 920-927.
29. H. Duan, S. Nie , *J. Am. Chem. Soc*. 2007 **129**, 3333-3338.
30. Y. Zhang, A. R. Clapp, *Sensors.*2010, **11**, 11036-11055.
31. F. Dubois, B. Mahler, B. Dubertret, E. Doris, C. Misoskowski, *J. Am. Chem. Soc*. 2007, **129**, 482-483.
32. Y. Zhang, A. M. Schnoes, A. R. Clapp, *ACS Appl. Mater. Interfaces*. , 2010, **2**, 3384-3395.
33. Y. Li, B. Shen, L. Liu, H. Xu, X. Zhong, *A Physiochemical and Engineering Aspects.*, 2012, **410**, 144 -152.
34. B.A. Tannous, J. Grimm, K. F. Perry, J. W. Chen, R. Weissleder, X. O. Breakefield, *Nat. Methods.*, 2006, **3**, 391-396.
35. H. Sakahara, T. Saga., *Adv. Drug. Deliv. Rev.*, 1999, **37**, 89-101.
36. G. Paganelli, *Eur.J. Nuel. Med.*, 1992, **19**, 322-329.
37. H. Kobayashi, S. Kawamoto, R. A. Star, T. A. Waldmann, M. W. Brechbiel, P. L. Choyke, *Bioconjugate Chem.*, 2003, **14**, 1044-1047.
38. G. F. V. Tilborg, *Magn. Reson. Med.*, 2008, **60**, 1444-1456.
39. R. P. Chauhan, G. Singh, S. Singh, N. Bag, M. Patra, S.A. Vadera, A.K. Mishra, R. Mathur, *Cancer Nano*., 2011,**2**, 111-120.
40. H. Rong, Y. Xiaogang , T. Hongye, G. Feng, C. Daxiang, G. Hongchen, *Front. Chem. China.*, 2006,**4**, 378-383.
41. K. W. Cai, Z. Chen, Z. Li, S. S. Gambhir, X. Chen, *J. Nuc. Med.*, 2010, **48**, 1862-1870.
42. M. L. Schipper, Z. Cheng, S. W. Lee, *J. Nuc. Med.*, 2007, **48**, 1511-1518.
43. W. Cai, D. W. Shin, K. Chen,. *Nano. Lett.*, 2006, **6**, 669-676.
44. W. J. Mulder, R. Koole, R. J. Brandwijk, *Nano. Lett*., 2006, **6**, 1-6.
45. V. S. Talanov, C. A. Regino, H. Kobayachi , M. Bernardo, P. L. Choyke, M. W. Brechbiel, *Nano. Lett*., 2006,**6**, 1459-1463.
46. R. Weissleder, A. Bogdanove, E. A. Neuwelt, M. Papisov, *Adv. Drug. Deliv. Rev.*, 1995, **16**, 321-334.
47. C. Sun, J. S. H. Lee, M. Zhang, *Adv. Drug. Deliv. Rev.*, 2008, **60**, 1252-1265.
48. S. F. Rosebrough, *Nucl. Med. Biol*., 1993, **20**, 663-668.
49. X. Wu, F. Tian, J. X. Zhao, M. Wu, *Expert. Opin. Drug Metab. Toxicol.*, 2013, **9**(11), 1265-1277.